OXFORD GENETICS

GENETICS, 2024, 227(4), iyae087
https://doi.org/10.1093/genetics/iyae087
Advance Access Publication Date: 28 May 2024
Investigation

Posttranscriptional regulation of the T-box gene *midline* via the 3′UTR in Drosophila is complex and cell- and tissue-dependent

Kalpana Makhijani,[1] Jordan Mar,[1] Ivana Gaziova,[2] Krishna Moorthi Bhat [1,2,3,4,*]

[1]Department of Molecular Medicine, University of South Florida, Tampa, FL 33613, USA
[2]Department of Neuroscience and Cell Biology, University of Texas Medical Branch School of Medicine, Galveston, TX 77555, USA
[3]Department of Biomedical Engineering, Heersink School of Medicine and School of Engineering, University of Alabama at Birmingham, Birmingham, AL 35233, USA
[4]Department of Neurology, Heersink School of Medicine, University of Alabama at Birmingham, Birmingham, AL 35233, USA

*Corresponding author: Department of Biomedical Engineering, Heersink School of Medicine and School of Engineering, University of Alabama at Birmingham, 1825 University Blvd, Birmingham, AL 35233, USA; Department of Neurology, Heersink School of Medicine, University of Alabama at Birmingham, 1825 University Blvd, Birmingham, AL 35233, USA. Email: bhatk@uab.edu

The T-box (Tbx) proteins have a 180–230 amino acid DNA-binding domain, first reported in the Brachyury (T) protein. They are highly conserved among metazoans. They regulate a multitude of cellular functions in development and disease. Here, we report posttranscriptional and translational regulation of *midline* (*mid*), a Tbx member in Drosophila. We found that the 3′UTR of *mid* has mRNA degradation elements and AT-rich sequences. In Schneider S2 cells, *mid*-mRNA could be detected only when the transgene was without the 3′UTR. Similarly, the 3′UTR linked to the Renilla luciferase reporter significantly reduced the activity of the Luciferase, whereas deleting only the degradation elements from the 3′UTR resulted in reduced activity, but not as much. Overexpression of *mid* in MP2, an embryonic neuroblast, showed no significant difference in the levels of *mid*-mRNA between the 2 transgenes, with and without the 3′UTR, indicating the absence of posttranscriptional regulation of *mid* in MP2. Moreover, while elevated *mid*-RNA was detected in MP2 in nearly all hemisegments, only a fifth of those hemisegments had elevated levels of the protein. Overexpression of the 2 transgenes resulted in MP2-lineage defects at about the same frequency. These results indicate a translational/posttranslational regulation of *mid* in MP2. The regulation of ectopically expressed *mid* in the wing imaginal disc was complex. In the wing disc, where *mid* is not expressed, the ectopic expression of the transgene lacking the 3′UTR had a higher level of *mid*-RNA and the protein had a stronger phenotypic effect. These results indicate that the 3′UTR can subject *mid*-mRNA to degradation in a cell- and tissue-specific manner. We further report a balancer-mediated transgenerational modifier effect on the expression and gain of function effects of the 2 transgenes.

Graphical Abstract

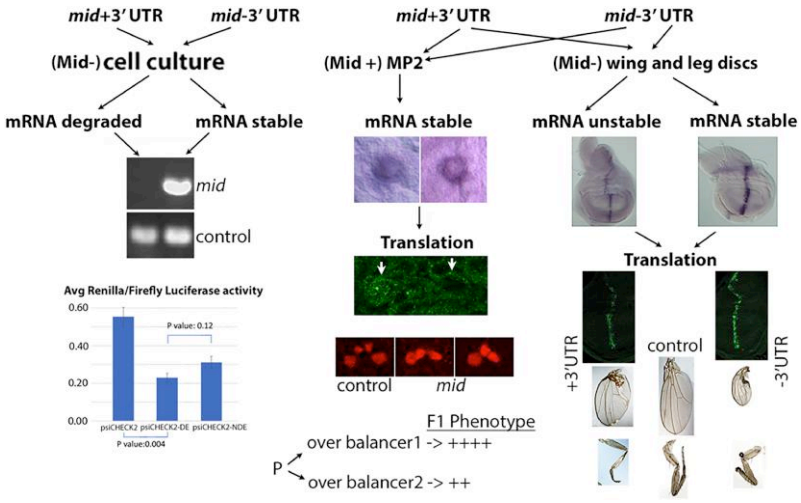

Keywords: Drosophila; cell culture; transcription; experimental technology; *midline* gene; 3′UTR; genetics

Received on 01 April 2024; accepted on 17 May 2024

Introduction

The members of the T-box (Tbx) family of proteins are highly conserved among metazoans and are defined by the presence of a 180–230 amino acid DNA-binding domain called the T-box domain. The name T-box derives from the presence of this domain discovered initially in the Brachyury (T) protein. Several studies in vertebrates show that T-box proteins are important, regulating a multitude of cellular processes in development and disease across species (Nusslein-Volhard *et al.* 1984; Kolodziej *et al.* 1995; Bamshad *et al* 1997; Li *et al.* 1997; Basson *et al.* 1999; Merscher *et al.* 2001; Qian *et al.* 2005; Gaziova and Bhat 2009; Manavalan *et al.* 2013; Gaziova *et al.* 2020; Amor-Salamanca *et al.* 2024). In vertebrates, the loss of function in Tbx genes such as *midline* (*mid*) and *H15* causes ectodermal defects (Nusslein-Volhard *et al.* 1984; Manavalan *et al.* 2013), heart defects (Qian *et al.* 2005), neuronal identity specification defects (Kolodziej *et al.* 1995; Gaziova and Bhat 2009; Manavalan *et al.* 2013), and cell division defects (Gaziova *et al.* 2020). In humans, the Holt–Oram syndrome with upper limb malformation and congenital heart disease is caused by haploinsufficiency of *TBX5* (Li *et al.* 1997; Basson *et al.* 1999). Recently, a rare haploinsufficiency of *TBX20,* which is an orthologue of Drosophila *mid* gene, was shown to cause dilated cardiomyopathy and left ventricular noncompaction (Amor-Salamanca *et al.* 2024). Haploinsufficiency of the mouse *Brachyury* and human *TBX3* and *TBX1* genes produces dominant phenotypes such as short or missing tails, Ulnar–Mammary syndrome, and DiGeorge syndrome (Bamshad *et al.* 1997; Merscher *et al.* 2001). Thus, dosage sensitivity appears to be one of the striking attributes of Tbx proteins. TBX3 and TBX1 are also required for breast development, and mutations in TBX3 cause breast cancers (Chang *et al.* 2016). Studies also indicate that TBX2 and TBX3 suppress replicative senescence, while TBX3 cooperates with Myc and Ras in cellular transformation and inhibits apoptosis (Carlson *et al.* 2002). Similarly, TBX2 binds and represses the p21 promoter in vitro and in vivo (Prince *et al.* 2004), and binds to the p21WAF1 Cyclin-dependent kinase inhibitor, which plays a key role in senescence and cell-cycle arrest after DNA damage.

In the Drosophila nerve cord, about 10,000 neurons are generated by about 1,000 primary neuroblast (NB) stem cells. These primary NBs undergo a self-renewing asymmetric division to generate secondary precursors called Ganglion Mother Cells or GMCs (Doe 1992). GMCs divide only once to generate 2 distinct postmitotic neurons. There is an NB called MP2, and while formed as an NB under the regulation of neurogenic and proneural genes, it behaves like a GMC, dividing only once to generate 2 neurons called vMP2 and dMP2 (Doe 1992; Gaziova *et al.* 2020). Our recent results showed that Mid is transiently expressed at low levels in MP2 and loss of function for *mid* causes MP2 to behave like a multipotential NB, dividing more than once to generate additional v and dMP2 neurons (Gaziova *et al.* 2020). Moreover, we showed that Mid is involved in repressing the *cyclin E* promoter. These results highlight its potential role in cell division, cell transformation, cell-cycle arrest, and senescence, processes where the level and expression dynamics are critical.

In general, protein levels are regulated at the transcriptional and posttranscriptional levels. In this work, we show that *mid* is regulated at the posttranscriptional level. The posttranscriptional level regulation was very tight in Schneider S2 cells, where *mid* is not expressed and was mediated by the 3′UTR carrying the well-known mRNA degradation elements. In embryos, translational/posttranslational regulation of *mid* appears to be present in MP2, where *mid* is expressed at low levels (Gaziova *et al.* 2020), but post-transcriptional mRNA degradation was not observed. In the wing disc where *mid* is not normally expressed, the ectopically expressed *mid* gene was regulated via the 3′UTR. However, this regulation was not as tight as in S2 cells. Consistent with these results were also the phenotypes such as lethality or wing and leg defects. Interestingly, the phenotypes were significantly impacted by a transgenerational modifier effect of balancer chromosomes. These results provide important insights into the regulatory aspect of a gene that is involved in development and disease across metazoans.

Materials and methods

Fly stocks and genetics

The *mid* mutant alleles used were mid^{1} and a deficiency that removes both *mid* and *H15* genes (*mid*, $H15^{df}$ or mid^{df}; Bl# 7498; breakpoints: 25D5-25E6). The other lines used were as follows: *ac*-GAL (BL#: 8715), UAS-*mid*-C3 (with the 3′UTR), UAS-*mid*-72L (without the 3′UTR), AJ96-LacZ (Gaziova *et al.* 2020), *ptc*-GAL4/Cyo, KrGAL4, UAS-GFP, *ptc*-GAL4/InGlaBc, and *mid*: PBac{*mid* GFP.FPTB}VK00031 (BN Stock # 96800). For the wild type, we used Oregon R flies. To induce *mid*-RNAi in the *ptc*-domain in the wing or leg discs, we used the RNAi line HMC03082 (BN#50681) from TRiP and the *ptc*-GAL4 line. The inductions were done at different temperatures including at 29°C. Standard genetics were used to obtain combinations of genotypes wherever needed.

Generating transfection constructs and transgenic lines with and without the 3′UTR

A full-length *mid*-cDNA clone carrying the 3′UTR (DGRC; #8892; 2,960 bp) was sequenced. We identified 2 silent single-nucleotide mutations in positions 1,799 and 1,946, this segment was replaced by MscI (1742)—HpaI (2022) PCR fragment amplified from genomic DNA. This full-length *mid*-cDNA was then cloned to the pBluescript KS + (Strategene) and used for generating the constructs for transfection assays as follows: To express full-length cDNA in Drosophila cell culture, the cDNA with the 3′UTR was subcloned to the vector pAc5.1/V5-His A (Life Technologies). This will provide a high-level and constitutive expression of the Mid protein since the expression in this vector is driven by a strong, constitutive Drosophila *actin* 5C gene promoter. For the inducible expression of the same full-length cDNA, it was subcloned into the expression vector pMT/V5-His A (Life Technologies). This system uses the Drosophila *metallothionein* gene promoter, which can be induced in S2 cells upon addition of copper sulfate.

To remove the 3′UTR region from *mid*-cDNA, the STOP codon was replaced by the XbaI restriction site and fused with His sequence in either the pAc5.1/V5-His A or the pMT/V5-His A, respectively, using KpnI and XbaI restriction sites. A total of 4 constructs for transfection were generated, as follows: (1) *actin*-promoter-fused to the full-length *mid*-cDNA along with the 3′UTR, (2) *actin*-promoter-fused to the full-length *mid*-cDNA lacking the 3′UTR region, tagged with His tag, (3) *metallothionein*-promoter-fused to the full-length *mid*-cDNA along with the 3′UTR, (4) *metallothionein*-promoter-fused to the full-length *mid*-cDNA lacking the 3′UTR region, tagged with His tag. For generating Drosophila transgenic lines, the pUAST-*mid* + 3′UTR construct was generated as previously published (Gaziova and Bhat 2009), by subcloning the entire *mid*-cDNA (RE27439; Berkeley Drosophila Genome Project) into the pUAST P-element vector. The pUAST-*mid* 3′UTR construct was made by introducing an XbaI restriction site immediately behind the stop codon in the original *mid*-clone and by subcloning it into the pUAST P-element vector. The transgenic lines were generated using

the standard Drosophila transgenic protocols. All the transgenes were sequenced before transfection or before and after generating transgenic lines to ensure that there were no errors in the transgenes that might affect the expression.

Cell culture, transfection, and transient expression assays

Drosophila S2 cells (Life Technologies) were grown in Shields and Sang Medium (Sigma) with 10% FBS at 25°C. For transient transfection experiments, S2 cells were seeded in 10 cm plates and transfected 24 h later at 30–50% confluency using the calcium phosphate transfection method [for detailed protocol, see (Gaziova and Bhat 2009)]. For constitutive expression, S2 cells were transfected with either the pAc5.1-*mid* 3′UTR or the pAc5.1-*mid*-His, respectively, and cells were collected 24, 48, and 72 h after the transfection for RNA isolation. For inducible expression, S2 cells were transfected with either the pMT-*mid* 3′UTR or the pMT-*mid*-His, respectively, and 24 h after the transfection, media was replaced and the *metallothionein* gene promoter was activated with 50 µM copper sulfate for 2, 4, and 6 h. Total RNA was isolated using the TRIzol Reagent (Life Technologies) and the first-strand cDNA was synthesized using SuperScript III First-Strand Synthesis System (Life Technologies) according to the manufacturer's protocol. *mid* gene RNA was assayed using 5-CGTCGTCGCCTGCCTTCCG-3 (forward) and 5-CTGGAACATGTGGAAGGCG-3 (reverse) primers. As an endogenous positive control, the *slit* gene was chosen and detected using 5-CCATATGCGTAACCAGCTGAAGGAGATACC-3 (forward) and 5-GAAGCTTTCAGGTCAACGACTTGAGGTCC-3 (reverse) primers.

Mid 3′UTR analysis using the luciferase activity assay

Dual luciferase reporter cloning

The 3′UTR sequence (following stop codon) from the *mid*-transcript-L was synthesized and cloned into the XhoI and NotI sites in the multiple cloning region downstream to the translational stop codon of Renilla luciferase in psiCHECK2 dual luciferase reporter vector from Promega (GenScript gene synthesis service). This plasmid was named psiCEHCK2-DE, where DE stands for degradation element (see Supplementary Fig. 2, File 1). A *mid* 3′UTR sequence in which the color-highlighted degradation elements were deleted was synthesized and cloned into the XhoI and NotI sites in the psiCHECK2 vector. This plasmid is named psiCHECK2-NDE, where NDE stands for no degradation element (see Supplementary Fig. 2, File 1).

S2 cell transfection

S2 cells were purchased from Thermofisher Scientific and were cultured in complete Schneider's Drosophila medium containing 10% heat-inactivated FBS and Penicillin–Streptomycin. The S2 cells were seeded at a concentration of 1×10^6 cells/well in 6-well plates prior to the day of transfection and incubated at 25°C. Following overnight incubation, the cells were transfected individually with psiCHECK2, psiCHECK2-DE, and psiCHECK-NDE using the TransIT insect transfection reagent from Mirus. As a negative control, one of the wells containing S2 cells was treated with a transfection reagent without any plasmid DNA.

Luminescence assay

The dual luciferase reporter assay was performed 48 h after transfection by recovering the cells from the 6-well plates by several rounds of pipetting up and down and transferring 75 µL cell suspension to a white solid bottom 96-well plate. The luminescence assay was performed using the Dual glow luciferase system (cat. no. E2920 Promega) in triplicate per the manufacturer's instructions, and the firefly and Renilla luminescence were measured using the Glowmax Discover microplate reader. The S2 cells with no transfection were used for the measurement of background Renilla and firefly luminescence, which was subtracted from the experimental luminescence values. A ratio of Renilla/firefly luciferase was determined, and the average of the triplicates was plotted and shown in the figure. The error bars shown in the graph are SEM.

Immunohistochemistry, whole-mount RNA in situ analysis, and GFP imaging

The embryo collection, fixation, and immunostaining were performed according to the standard procedures. Briefly, for immunolabeling, embryos were washed thoroughly with running water, dechorionated with 50% bleach, rinsed with running water, and then with phosphate-buffered saline containing 0.1% Triton X-100 (Sigma) and fixed in equal volumes of *n*-heptane and 37% formaldehyde (Fisher Scientific) for 2 min (immunofluorescence labeling) or 6 min (immunohistochemical labeling). Vitelline membranes were removed by a rapid (~20 s) wash with methanol (Fisher Scientific). Embryos were processed immediately. The following antibodies were used: anti-Mid (rat, 1:50; Gaziova and Bhat 2009), anti-Odd (guinea pig, 1:100, John Reinitz), anti-β-galactosidase (mouse, 1:500; Cappel; rabbit 1:500, Molecular Probes), and anti-β-galactosidase (rabbit; 1:3,000, Invitrogen, A-11132, or mouse, 1:400; DSHB, 40-1a). For color visualization, either AP-conjugated or horseradish peroxidase (HRP)-conjugated secondary antibodies were used. For light microscopy, secondary antibodies conjugated to alkaline phosphatase (rabbit, 1:200, Pierce, 31341) or HRP (rabbit, 1:200, Pierce, 31460) were used. Alkaline phosphatase was detected using 5-bromo-4-chloro-3-indolyl-phosphate and nitroblue tetrazolium (Promega, S3771). HRP was detected with diaminobenzidine (Sigma, D4418). For confocal visualization, secondary antibodies conjugated to Cy5 (rabbit, 1:400, Invitrogen, A10523), fluorescein isothiocyanate (mouse, 1:50, Invitrogen, 62-6511), Alexa Fluor 488 (rabbit or mouse, 1:300, Invitrogen, A-11008 or A-11001), Alexa Fluor 647 (rabbit or mouse, 1:300, Invitrogen, A-21245 or A-21236), or Alex Fluor 633 (1:400) were used.

For immunostaining of larval imaginal discs, third instar larvae were dissected and turned inside out in cold PBS and fixed in 4% paraformaldehyde for 20 min. The fixed larvae with the imaginal discs attached were washed with PBS and were incubated in PBS containing 0.1% TritonX-100 and 10% NGS for 2–3 h for permeabilization and blocking. The larvae were then incubated with the primary antibody diluted in PBS containing 0.1% TritonX-100 and 10% NGS overnight at 4°C. The larvae were washed with PBS containing 0.1% TritonX-100 (PBS-T) 3–4 times with 20 min for each wash then incubated in a secondary antibody diluted in PBS-T + 10% NGS [Alexa Fluor 488 (1:400)] for 2 h at room temperature. The larvae were washed with PBST, and the imaginal discs were dissected and mounted in Vectashield for imaging.

RNA in situ hybridization was performed using the Digoxigenin labeled antisense RNA for *mid*. The antisense RNA probe was synthesized using the in vitro transcription of the linearized *mid*-cDNA in the Bluescript vector. The hybridization of larval imaginal discs and embryos was done as described previously (Tautz and Pfeifle 1989; Wilk *et al.* 2017). Fluorescent images were collected using confocal microscopy (BioRad confocal and Zeiss LSM880). For mid-GFP imaging, the wing imaginal discs were dissected from PBac{*mid* GFP.FPTB} fly stock in PBS and mounted in Vectashield medium containing DAPI on a glass slide with spacers. The GFP and

DAPI images were collected every 1 μm (see Supplementary Fig. 5, File 1).

qPCR analysis

The third instar larval progeny was collected from the following crosses set at 18°C and 20°C: *ptc*-GAL4/CyO-Kr-GAL4, UAS-GFP × UAS-*mid* (+3′UTR) and *ptc*-GAL4/CyO-KrGAL4, UAS-GFP × UAS-*mid* (−3′UTR). Wing discs were dissected from the third instar stage larvae that were GFP negative. All materials used were treated with Apex RNase Free Surface Decontaminant (Genesee Scientific) before use. Dissected wing discs were collected into a BioMasher II Tube containing 100 μL sterile 1× PBS. PBS was removed and wing discs were homogenized in an extraction buffer consisting of Buffer RLT (Qiagen) supplemented with 80 μM DTT on ice. Wing disc lysate was transferred to QIAshredder column (Qiagen) and centrifuged at max speed for 3 min. The temperature of the centrifuge was set to 25°C for this and all subsequent centrifugations. The flow-through from this step was used to isolate RNA using the RNeasy Mini Kit (Qiagen) following the manufacturer's directions. Isolated RNA was quantified using NanoDrop 2100 Spectrophotometer (ThermoFisher). Three biological replicates were made for each genotype and temperature condition. The concentration and purity of the RNA were assessed using a NanoDrop 2000 Spectrophotometer (ThermoFisher). iScript cDNA Synthesis Kit (Bio-Rad) was used to generate cDNA from 150 ng RNA for every sample. cDNA was then diluted 1:10 using RNase-Free Water (Qiagen) and stored at −20°C until use. qPCR reactions were assembled in a 96-well plate (Roche) and consisted of primers (final concentration: 500 nM/reaction), cDNA (500 ng/reaction), and FastStart Essential DNA Green Master (Roche). The plate was sealed, briefly centrifuged, then loaded into an Azure Cielo 6 Real-Time PCR machine (Azure Biosystems) and ran. The *mid*-gene expression was normalized to rpl32 expression. For each genotype, 3 biological replicates were averaged to obtain the final value. One sample from the 20°C ptc/*mid* (−3′UTR) group was discarded owing to inconsistent rpl32 Ct values. qPCR data were arranged into a spreadsheet and then analyzed using the delta-delta CT method (Livak and Schmittgen 2001). The *mid* and *rpl32* primers used for this experiment include AACAACA ACGGCTAGCAAAAGT (F) and CGACCACATCAACGTCAACCT (R), rpl32-F: AGCATACAGGCCCAAGATCG (F), and TGTTGTCGAT ACCCTTGGGC (R). Sequences are provided in 5′ to 3′ directions and were synthesized by Eurofins.

ImageJ analysis/fluorescent intensity measurement

We used the plot profile function in ImageJ to determine the level-distribution profile of the expression of Mid (Fig. 2). The following steps were adopted: images were saved as 300-pixels/Inch resolution in Adobe Photoshop, and then converted into JPEG files. The JPEG images were opened with ImageJ with the following measurement setup: Area, mean gray value, and integrated density were set under Measurements. Using the rectangle function, the area in the cell was defined, and under Analyze, the Plot profile function was used for analysis. Since the expression of Mid in one group of MP2 was the baseline, we did not convert the gray values into numbers, therefore no statistics were applied (this is like a 0 vs >0 situation). For ImageJ analysis shown in Fig. 6, we adopted a slightly different methodology (see Supplementary Fig. 6, File 1). Briefly, the fluorescent intensity for Mid-immunostaining on wing imaginal discs was determined as follows: a rectangular region of interest (ROI) was selected in the patched GAL4-driven Mid-expressing region in the wing pouch, and the fluorescent intensity or the area integrated density was determined. The area of the ROI was kept the same for different samples. The background intensity was determined for each imaginal disc by selecting a rectangular ROI of the same size in the non-Mid-expressing region and was subtracted from the intensity in the Mid-expressing domain. The number of wing imaginal discs analyzed for fluorescent intensity measurements was 16 to 19 per genotype.

Statistics

We used a 2-tailed 2-sample equal variance Student's *t* test for determining the statistical significance of Mid immunofluorescence intensity and qPCR data. For the luciferase activity assay, we used a 2-tailed 2-sample equal variance test. See Supplementary data for the datasets.

Results

The *mid* gene has mRNA degradation elements in its 3′UTR and is tightly regulated in the Drosophila Schneider S2 cells

Our previous work indicated that *mid*-expression in NB stem cells such as MP2 is highly dynamic (Gaziova *et al.* 2020), but in certain other NBs, it was expressed at high levels without a strong regulation (Gaziova and Bhat 2009; Manavalan *et al.* 2013). To explore the molecular basis for this differential regulation, we examined the 3′UTR of *mid*. The *mid* locus appears to generate 2 different transcripts, one with a long 3′UTR and the other with a short 3′UTR (Flybase, see Supplementary Fig. 1, a and b, File 1). The 3′UTR of the long *mid*-transcript (*mid*-transcript-L) had a total of 11 mRNA degradation sequence motifs. These are 5 AUUUA motifs, 5 GACUAA motifs, and one Bearded (Brd) box motif (Fig. 1a, Supplementary Fig. 1a, File 1). Additionally, the 3′UTR of *mid* is also very AT-rich, whereas the short 3′UTR *mid* has only one degradation element (Supplementary Fig. 1b, File 1). Several mRNAs that are regulated posttranscriptionally have these elements (Savant-Bhonsale and Cleveland 1992; Lai and Posakony 1997).

To determine if these motifs are involved in the regulation or degradation of *mid*-mRNA, we used the Drosophila Schneider S2 cells in transient transfection assays. Neither *mid,* nor its closely related Tbx gene, *H15*, which is located next to *mid* (Gaziova and Bhat 2009), are expressed in the S2 cells. We generated *mid*-constructs with and without the 3′UTR under the control of *actin* (*act*) or *metallothionein* (*MT*) promoters. These *mid*-constructs were transfected to Schneider cells and expressed either constitutively from the *actin* promoter or induced from the *MT* promoter by adding copper sulfate to the media. The total mRNA was prepared from these cells after 24, 48, and 72 h of transfection, or 2, 4, and 6 h after inducing the *MT* promoter by infusing the media with copper sulfate. The expression of *mid* was determined in these samples using RT-PCR. As shown in Fig. 1, b and c, we did not detect any amplified *mid*-DNA products in cells transfected with the *mid*-transgene containing the 3′UTR. However, the *mid*-gene product was readily detected in S2 cells transfected with the transgene without the 3′UTR. These results indicated that *mid*-mRNA was tightly regulated posttranscriptionally at the mRNA degradation level in S2 cells.

To obtain additional evidence for the *mid* 3′UTR-mediated regulation of mRNA degradation and also to confirm the role of the 3′UTR-degradation elements (see Fig. 1a) in this regulation, we generated plasmids containing the 3′UTR with and without deletions of all the degradation elements downstream to the translation stop codon of the Renilla *luciferase* reporter gene

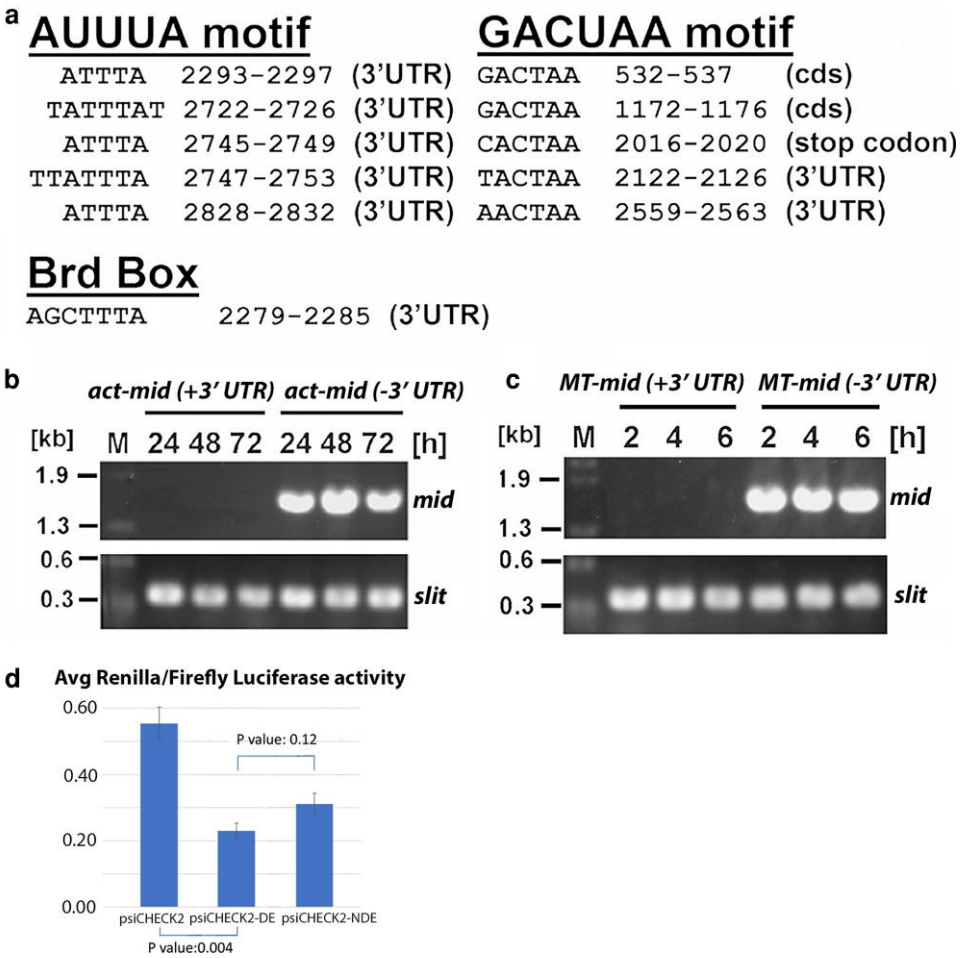

Fig. 1. The *mid*-transcript carrying the 3′UTR with its mRNA-degradation elements was completely degraded in Schneider S2 cells. a) The 3′UTR of *mid* contains mRNA-degradation elements. Brd, Bearded, cds, coding sequence (see Supplementary data for the 2 different *mid*-transcripts). b, c) RT-PCR analysis of mRNA isolated from Drosophila Schneider S2 cells after the transfection with *actin* (*act*)-*mid* or *metallothionein* (MT)-*mid* with the 3′UTR and without the 3′UTR. The MT transgene was induced by replacing the media with 50 μM copper sulfate for 2, 4, and 6 h. The *slit* gene was used as a control for transfection and RT-PCR analysis. M denotes molecular size markers in kilobase (kb). d) Dual-luciferase reporter assay shows that the *mid* 3′UTR reduces the stability of Renilla luciferase. The graph shows the average ratio of Renilla/firefly luminescence in S2 cells 48 h after transfection with psiCHECK2 (vector only), psiCHECK2-DE (with degradation elements), and psiCHECK2-NDE (without the degradation elements). Error bars indicate standard error.

(psiCHECK2-DE and psiCHECK2-NDE; see Fig. 1a, Supplementary Fig. 2, File 1, Materials and Methods). The S2 cells were transfected individually with the plasmids psiCHECK2, psiCHECK2-DE, and psiCHECK-NDE and, dual luciferase reporter assay was performed 48 h after transfection to measure the firefly and Renilla luminescence. The S2 cells with no transfection were used for measurement of background Renilla and firefly luminescence, which was subtracted from the experimental luminescence values. A ratio of Renilla/firefly luciferase was determined, and the average of the triplicates was plotted as shown in Fig. 1d. We found that the Renilla activity was significantly reduced in cells transfected with the 3′UTR containing the degradation elements (psiCHECK2-DE) compared with the plasmid control, which is consistent with the results shown in Fig. 1, b and c. However, while the activity was increased in cells transfected with the plasmid carrying the 3′UTR that had the deletions of the degradation elements (psiCHECK2-NDE), the increase was not highly significant (Fig. 1d). This result suggests that the highest level of *mid*-RNA degradation mediated by the 3′UTR requires all of the 3′UTR (Fig. 1a). This is consistent with the fact that the 3′UTR is enriched with AT sequence (see Supplementary Fig. 1a, File 1). These results are important since they provide insights not just into the *mid*-RNA degradation, but also degradation of other RNAs, i.e. that the RNA degradation can involve more than the known degradation elements, all of the 3′UTR could be involved.

The endogenous *mid*-expression is regulated in a cell-specific manner in the embryonic nerve cord

We next explored if *mid* is regulated at the mRNA-degradation level in the embryonic nerve cord since the expression of Mid in the CNS appears to be regulated (Gaziova and Bhat 2009; Manavalan *et al.* 2013; Gaziova *et al.* 2020). It is expressed at high levels in NBs such as NB7-1, 7-2, 7-4 of row 7, and 2-4 of row 2. However, it is expressed at lower levels in NB 7-3, 7-5, 6-1, and at even lower levels in MP2 and a few other NBs. The MP2 lineage is an atypical NB lineage as it is formed as an NB but behaves as a GMC to produce 2 different postmitotic neurons, vMP2 and dMP2 (Gaziova *et al.* 2020). Other NBs undergo multiple self-renewing divisions, each time generating a GMC, which then divides to generate 2 postmitotic neurons. We have recently shown that in MP2, the levels of Mid were regulated, with almost no expression in an early and smaller-sized MP2, but detectable levels in a middle-

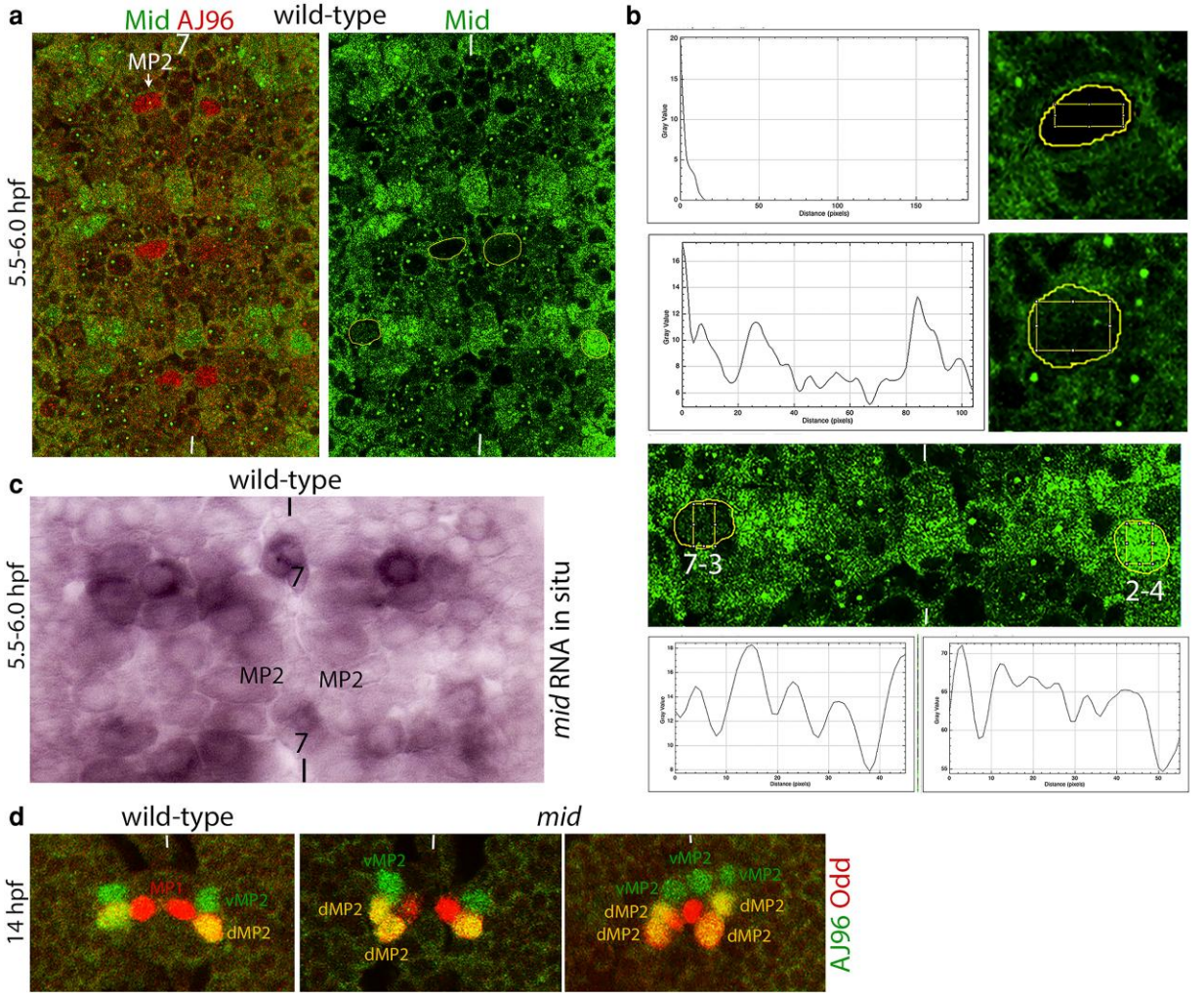

Fig. 2. Expression of Mid in MP2 and loss of function effects of *mid* on the MP2 lineage. The anterior end of the embryo is up, the midline is marked by the vertical line. Row 7 NBs are denoted with the number 7. a) Wild-type control embryos were double-stained for Mid and AJ96. AJ96 is an enhancer-trap line and is a marker for MP2. Images of the developing ventral nervous system are shown. b) Staining intensity plot profile across the yellow square using ImageJ analysis for the expression of Mid in MP2 (top 2 panels) and in NB7-3 and NB2-4 (bottom panel). In one group of MP2s, no detectable Mid was found (top panel), in the other, punctate staining for Mid was seen (middle panel). The expression of Mid in NB7-3 was also dynamic, whereas it was more or less constant and high in NB2-4 (bottom panel) (see Gaziova and Bhat 2009; Manavalan *et al.* 2013). c) Whole-mount RNA in situ for *mid* in the developing ventral nervous system. MP2 has low levels of *mid*-RNA. d) Wild-type control and *mid*-loss of function mutant embryos were double-stained for AJ96 and Odd. AJ96 is expressed in vMP2 and dMP2 neurons, and Odd is expressed in dMP2 (and in MP1, which is generated from a different NB lineage). In the mutant, hemisegments with 2 dMP2 and 1 vMP2 (middle and last panel) or 2 dMP2 and 2 vMP2 (last panel) were seen. Two vMP2 and 1 dMP2 were also seen in the mutant. See Gaziova *et al.* (2020) for the full analysis of *mid*-loss of function mutant phenotypes in MP2 lineage.

late larger-sized MP2. This is shown in Fig. 2 by double staining of wild-type control embryos with Mid and AJ96 (which is an enhancer-trap lacZ line active in MP2, as well as in vMP2 and dMP2 neurons) (see also reference Gaziova *et al.* 2020). The Mid-protein was absent in the smaller-sized MP2s from earlier-stage embryos, but the protein could be detected in larger-sized MP2s from later-stage embryos, before the division of MP2 (Fig. 2, a and b). Consistent with the protein expression, the level of *mid*-RNA in MP2 was also low (Fig. 2c). While the expression of Mid in MP2 was low, this low expression is functionally critical since our recent results showed that loss of function for *mid* causes MP2 lineage defects: MP2 undergoes self-renewing asymmetric divisions to generate extra v and d MP2 neurons (Gaziova *et al.* 2020; see also Fig. 2d). Thus, the regulation of levels of Mid in MP2 appears to be important and we determined the regulation of *mid* at the posttranscriptional level in MP2 (see the following).

A 3′UTR-mediated posttranscriptional regulation of *mid* does not occur in MP2 neuroblast in the embryonic nerve cord

We expressed the 2 *mid*-transgenes, with and without the 3′UTR, in MP2 to determine if *mid*-mRNA is regulated at the posttranscriptional level. We generated Drosophila transgenic lines carrying the *mid*-cDNA with 3′UTR or without it under the UAS promoter. Using the GAL4xUAS strategy (Brand and Perrimon 1993), these transgenes were induced in MP2 with the *achaete* (*ac*)-GAL4 driver. The *ac*-GAL4 is expressed in MP2 and is an effective driver of gene transcription in MP2. First, we examined MP2 in embryos expressing the 2 transgenes for *mid*-RNA by whole-mount RNA in situ. As shown in Fig. 3a, the level of *mid*-RNA, while low in wild-type control (see Fig. 2c), was increased with the induction of either of the transgenes. The expression levels of the transcript in MP2 were about the same for

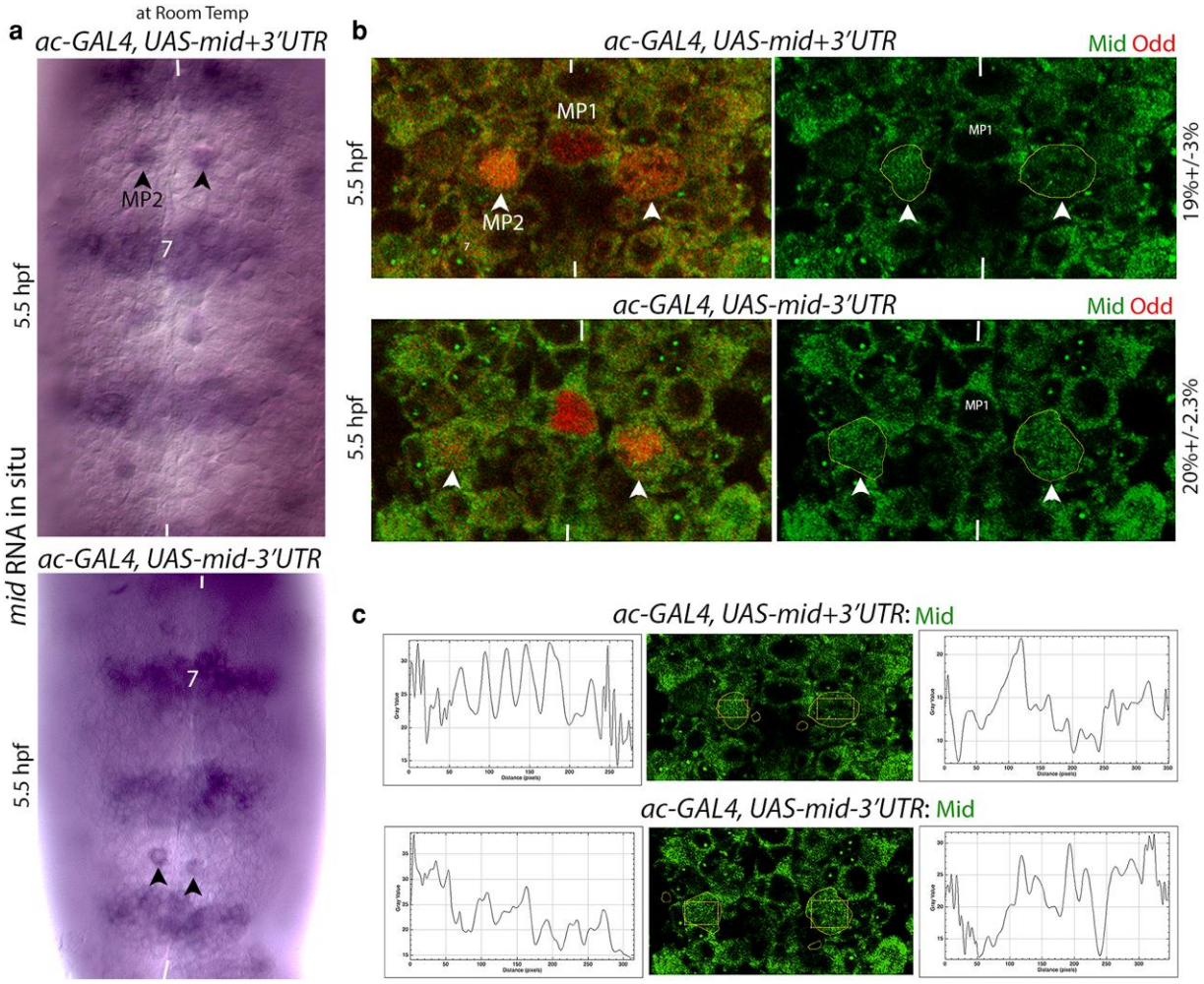

Fig. 3. Overexpression of *mid* with and without the 3′UTR in MP2. The anterior end is up, the midline is marked by the vertical line. Odd was used as a marker for MP2. Embryos were examined for the *mid*-RNA expression by whole-mount RNA in situ (a) and the protein expression, by immunohistochemistry (b, c) in MP2. ImageJ analysis was performed for the protein expression quantification in MP2 (c). The percentages with standard error in (b) represent the hemisegments expressing high levels of Mid. The *mid*-transgenes were induced by the *ac*-GAL4 driver. These experiments were done at room temperature (22°C). Mid is normally expressed at high levels in row 7 NBs.

the 2 transgenes, arguing that a 3′UTR-mediated posttranscriptional regulation of *mid* via mRNA degradation in MP2 is unlikely. More than one independent transgenic line for each construct showed similar results indicating that the results are not affected by the site of insertion.

Next, to determine the levels of the Mid-protein in MP2 in embryos expressing the 2 transgenes, embryos were double-stained for Mid and Odd-skipped (Odd), an MP2-marker (Gaziova *et al.* 2020). As shown in Fig. 3, b and c, the induction of the UAS-*mid* with or without the 3′UTR using the *ac*-GAL4 driver showed similar levels of the Mid-protein in MP2. Interestingly, in embryos expressing either of the 2 *mid*-transgenes, only about 19–20% of the hemisegments had higher than the normal levels of Mid in MP2: 19% ± 3% ($N = 60$ hemisegments) for the *mid*-transgene with the 3′UTR, and 20% ± 3% for the transgene without the 3′UTR ($N = 60$ hemisegments). In the remaining hemisegments, none to very low levels of the Mid-protein were seen with the 2 transgenes despite that >90% of the hemisegments ($N = 70$ hemisegments) had high levels of *mid*-RNA with the induction of either of the 2 transgenes (Fig. 3a). These results indicate that while there is no or very little 3′ UTR-mediated posttranscriptional degradation of the *mid*-RNA in MP2, there may be a translational or posttranslational regulation (degradation of the protein), mediating a down-regulation of Mid in MP2 in majority of the hemisegments. There may also exist a translational difference in MP2, where the 5′UTR represses the translation of both transcripts as a form of translational regulation specific to the *mid*-transcript. The 5′UTR of *mid* has many sites for RNA-binding proteins (RBPs) and those might mediate such a regulation (see Supplementary Fig. 3, File 1 for RBP sites in the 5′UTR of *mid*).

MP2-targeted overexpression of the *mid*-transgene with and without the 3′UTR causes a similar penetrance of the defects in the MP2 lineage

Our previous results showed that overexpression of *mid* in MP2 resulted in the misspecification, loss of division, and loss of MP2 progeny neurons, dMP2 and vMP2 (Gaziova *et al.* 2020). We compared the penetrance of the missing dMP2 defect between the 2 transgenes. This can be used as a functional readout or the measure of the effects of overexpression of the 2 transgenes in embryos. UAS-*mid*-transgenes with and without the 3′UTR were induced with *ac*-GAL4, and 14 hpf embryos were stained for Odd. At this stage, Odd is present only in

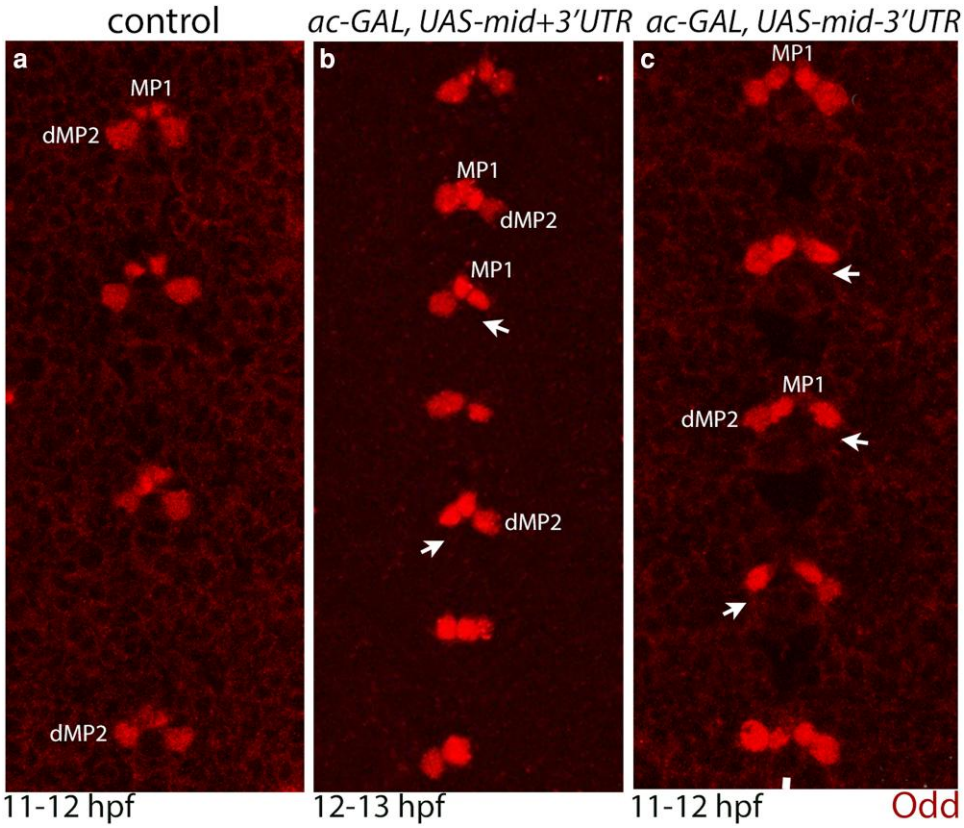

Fig. 4. MP2 lineage defects in embryos overexpressing *mid* with and without the 3′UTR in MP2. Control embryos (a) and embryos expressing the *mid*-transgene with the 3′UTR (b) or without the 3′UTR (c) in MP2 were stained for Odd, a marker for dMP2. They also stain a pair of MP1 neurons, which are generated by a distinct NB. Note the missing dMP2s (the position is marked by an arrow) with the overexpression of *mid*. The 2 *mid*-transgenes were induced by the ac-GAL4 driver. These experiments were done at room temperature (22°C).

dMP2 (and 2 MP1 neurons, which are from a different NB) (Fig. 4a). As shown in Fig. 4, b and c, the expression of either of the transgenes resulted in the loss of dMP2 neurons. The defects were seen in about 29.7% of the hemisegments ($N = 111$) for the transgene with the 3′UTR and 21.6% of the hemisegments ($N = 102$) for the transgene without the 3′UTR. These results indicate that the penetrance of the MP2 lineage defects roughly correlates with the percentage of hemisegments with high levels of Mid in MP2.

Mid regulation in the wing disc

Given the aforementioned results, we examined if the 3′UTR mediates posttranscriptional degradation of *mid*-RNA in wing discs in larval stages of development. While a previous study reported that wing discs have Mid-expression (Fu *et al.* 2016), we did not observe *mid*-RNA or Mid protein in these discs (Fig. 5a, Supplementary Fig. 4b, File 1, lower panel). However, we did detect Mid in the peripodial membrane of the wing disc (Supplementary Fig. 4b, File 1, upper panel; a few cells in the leg disc proper had Mid expression, Supplementary Fig. 5d, File 1) (see also Svendsen *et al.* 2015). To further examine the expression of *mid* in the wing disc, we used a genomic BAC construct that expresses GFP-tagged *mid*: PBac{*mid*-GFP.FPTB}VK00031 (BN Stock # 96800) and examined the expression in the wing imaginal disc. The larval wing imaginal discs were imaged for GFP and DAPI with confocal microscopy and a Z-series of images was collected every 1 μm of the wing disc. The confocal imaging showed that the nuclear expression of Mid-GFP protein was seen only in the overlying flat cells of the peripodial epithelium (Supplementary Fig. 5, File 1) similar to Mid immunostaining in IHC experiments (see Supplementary Fig. 4b, File 1, upper panel). Also consistent with the IHC, no nuclear GFP signal was detected in the disc proper cells of the wing disc (Supplementary Fig. 5b, File 1, see also Supplementary Fig. 4b, File 1, lower panel).

Finally, we obtained RNAi lines for *mid* (BN#50681, TRiP HMC03082) and then induced *mid*-RNAi in the wing disc using *patched* (*ptc*)-GAL4. The rationale is that if *mid* is expressed at very low levels, a loss of function through RNAi might cause a phenotype or defects in the wing. However, we did not observe any defects in the adult wing (or leg disc; cells in the *ptc*-domain do not normally express Mid) of these flies with *mid*-RNAi even at 29°C. There could be caveats, but these results are consistent with the finding that there is no significant Mid-expression or its requirements in the wing disc. It is possible that the antibody previous studies used may be cross-reacting to some other antigen.

Imaginal discs have a remarkable potential for cell division, and we reasoned that they might exert a tight posttranscriptional regulation of *mid*-RNA through the 3′UTR in a gain-of-function situation as in S2 cells. We used the *ptc*-GAL4 driver to induce *mid*-transgenes since *ptc*-GAL4 induces UAS-linked genes in the wing and leg imaginal discs in a well-defined domain. Induction of *UAS-mid* with the *ptc*-GAL4 resulted in the expression of *mid*-RNA (Fig. 5b) and the Mid-protein (Fig. 6a, Supplementary Fig. 6, File 1) (see Fig. 7a for *ptc*-GAL4 induction domain using the LacZ gene). These results further indicate that *mid* is not

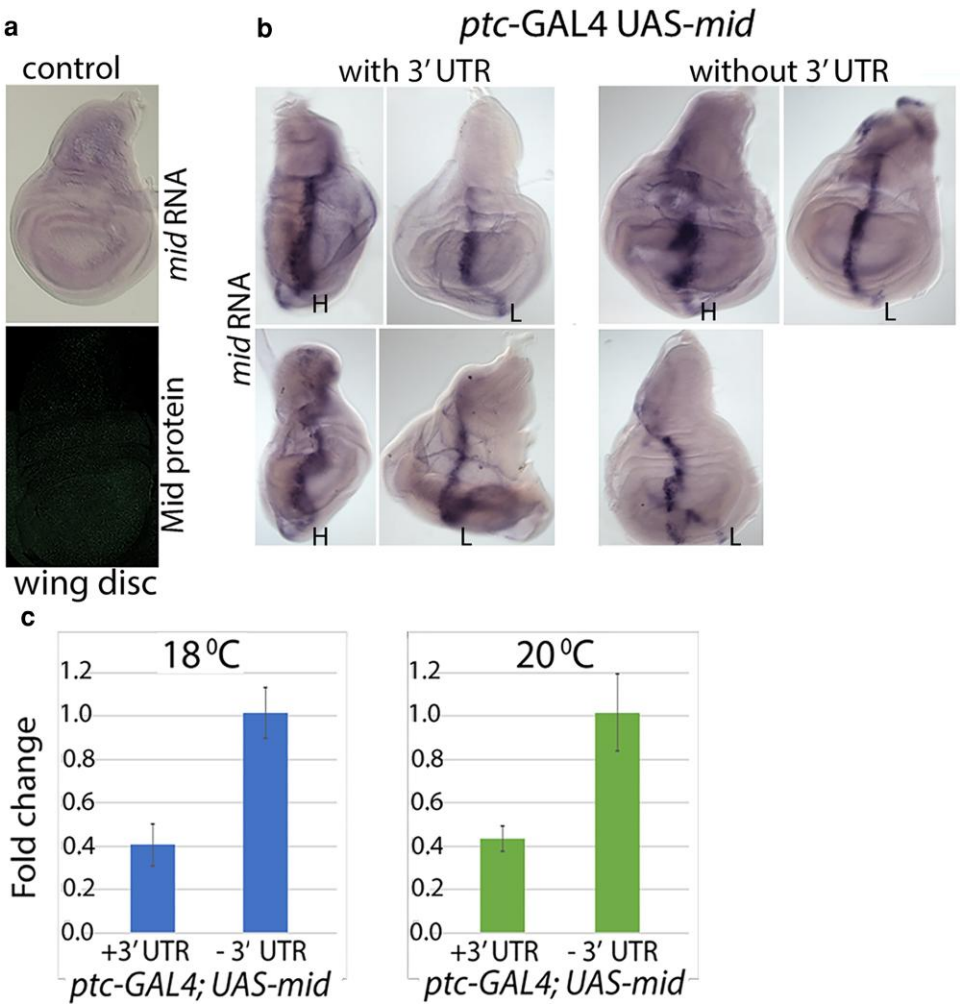

Fig. 5. Ectopic expression of *mid* with and without the 3′UTR in the wing disc. The *mid*-transgenes were induced by the *ptc*-GAL4 driver. a) Whole-mount *mid*-RNA in situ (top) and Mid-antibody immunohistochemistry (bottom) of the control wing disc without the *mid*-transgenes. No *mid*-expression was seen. b) Wing discs from third instar larvae expressing *mid*-transgenes with and without the 3′UTR raised at 20°C were analyzed for *mid*-RNA expression by whole-mount RNA in situ. Due to colorimetric-related variability with discs showing both high (H) and low (L) levels of *mid*-transgene expression with or without the 3′UTR, a qRT-PCR was performed. c) qRT-PCR for RNA isolated from discs expressing the *mid*-transgene with or without the 3′UTR from the *ptc*-GAL4 driver at 18°C and 20°C. Student's *t*-test was used for statistical significance. A significant difference ($P < 0.05$) in *mid*-expression was observed in both 18°C and 20°C conditions. We used data from 3 independent repeats.

endogenously expressed in the disc proper. A PCR-mediated detection would not be accurate since *mid* is expressed in the peripodial membrane of the discs (Supplementary Figs. 4b and 5b, File 1), and it will not be possible to separate the 2 groups of cells.

We induced the 2 transgenes with and without the 3′UTR at 29°C, 25°C, 22°C, 20°C, 19°C, and 18°C with *ptc*-GAL4 and found that induction at temperatures at and above 20°C caused fully penetrant embryonic lethality with both the transgenes. The driver *ptc*-GAL4 is also active in a subset of NBs in the embryonic nerve cord, in the embryonic ectoderm (Bhat 1996, 1999), as well as in the larval, pupal, and adult brain (Gaziova and Bhat 2009). Ectopic expression of *mid* in these cells/tissues may be the reason for the lethality. Furthermore, at higher temperatures, the GAL4 is much more active and induces UAS-linked genes at higher levels. This is likely the cause of the lethality at temperatures above 20°C. However, most of the lethality appears to occur during the pupal stage. Therefore, we sought to examine the expression of *mid*-RNA and the protein in the wing discs of the third instar larvae. First, we performed whole-mount RNA in situ of discs expressing *mid* with and without the 3′UTR in the *ptc*-domain. We found that after analyzing >30 discs using the colorimetric assay, it was not easy to discern the difference unless one picks and choses based on color development and is unblinded (Fig. 5b). That is to say that we found discs with both high (Fig. 5, b and h) and low (Fig. 5, b and l) expression of *mid*-RNA in 18°C or 20°C.

Since the colorimetric RNA-in situ analysis for quantitative purposes is not reliable, we performed qRT-PCR for *mid*-RNA from the discs where the UAS-*mid*-transgenes with and without the 3′UTR were induced by *ptc*-GAL4 at 18°C and 20°C temperatures. In both temperatures, there was an increase of about 2.5-fold when *mid* was lacking the 3′UTR, indicating that 3′UTR indeed mediates degradation of the transcript (Fig. 5c).

We next determined the levels of the Mid-protein in the wing disc expressing the 2 transgenes in the *ptc*-domain at 2 different temperatures by IHC (Fig. 6, a and b). The results showed that at 18°C, the difference in the levels of the Mid-protein between the 2 transgenes was not statistically significant although the discs expressing the transgene without the 3′UTR had higher levels of the protein (Fig. 6). However, the difference between the 2 was much higher and was statistically significant at 20°C (Fig. 6).

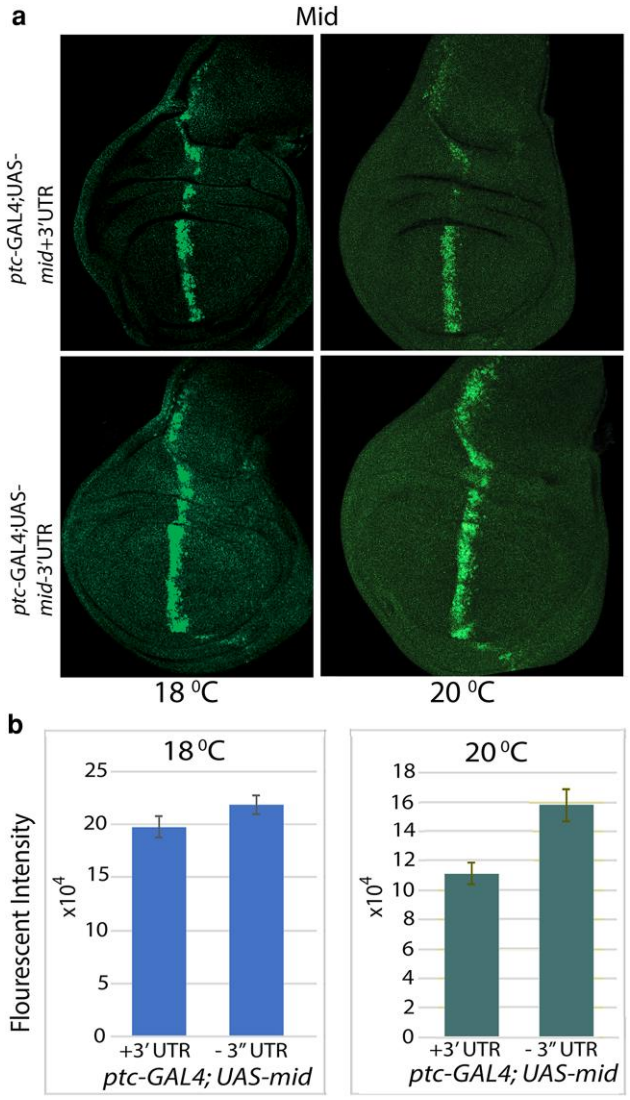

Fig. 6. The ectopic expression of the Mid-protein in wing disc from the *mid*-transgene with and without the 3′UTR at 18°C and 20°C. a) *Mid*-transgenes with and without the 3′UTR were induced by the *ptc*-GAL4 driver. The discs were analyzed for Mid-expression by an anti-Mid antibody. b) The intensity of signals was calculated using ImageJ analysis and represented as a histogram. We used 19 to 16 wing imaginal discs immunostained for the Mid-protein for intensity analysis for each genotype and temperature. The data were treated for statistical significance using the Student's "*t*" test. The difference at 18°C was not statistically significant ($P < 0.1$), whereas at 20°C the difference was statistically significant ($P < 0.001$).

Parental genotype affects the expression of the *mid*-transgenes

Previously, we had shown that there is a parental-balancer-mediated effect on the penetrance of the defects in the CNS in F1 progeny (Gaziova and Bhat 2009). Such effects can be interpreted as a transgenerational effect linked to balancer chromosomes. Balancer chromosomes carry many chromosomal aberrations such as a series of inversions, inversions within inversions, and duplications, such that they will not recombine with the homologous chromosome. Because of lack of recombination, they tend to also accumulate background and mostly recessive mutations. To determine if a balancer-mediated transgenerational effect might (differentially) modify the expression of the 2 transgenes, we moved the *ptc*-GAL4 driver to another second balancer chromosome called In(2LR), Gla, Bc from the original CyO balancer, *ptc*-GAL4/CyOKrGAL4, UAS-GFP. We then crossed this driver to UAS-*mid* with and without the 3′UTR. We found that the cross between *ptc*-GAL4/CyOKrGAL4, UAS-GFP, and UAS-*mid* with or without the 3′UTR caused lethality in the F1 generation, either at 18°C or 20°C, with no adults emerging (Table 1). When UAS-*mid* with the 3′UTR was crossed to *ptc*-GAL4/In(2LR), Gla, Bc at 18°C, we observed the emergence of the adults (27.9%), whereas UAS-*mid* without the 3′ UTR resulted in a much lower emergence of the adults (2.6%). At 20°C no adults emerged, with or without the 3′UTR (Table 1). Thus, the *mid*-transgene with the 3′UTR in this genetic combination was less toxic than without the 3′UTR. These results indicate that there is a transgenerational difference in the effects of *mid*-transgenes depending upon the parental genotype, in this case, the balancer-induced effects (see also Gaziova and Bhat 2009).

If the ectopic expression of Mid in the discs causes morphogenesis defects, a difference in the penetrance of the defects between the 2 transgenes might provide a functional confirmation of the aforementioned results. Therefore, the 2 transgenes were induced in the wing and leg discs using the *ptc*-GAL4 driver in both the balancer backgrounds at both 18°C and 20°C. The progeny were allowed to eclose into adult flies and their wing and legs were examined. As shown in Table 2, no adults emerged either at 18°C or at 20°C from either of the transgenes when the parental driver line was with the CyO balancer background. However, when the driver parental line was under the In (2LR) Gla, Bc background, and at 18°C, the transgene with the 3′UTR produced adults with 29% of them having a wing defect and 23% a leg defect (Table 2; Fig. 7). No adults emerged at 20°C (see Table 1). The transgene without the 3′UTR had very few adults emerge and 50% of them had wing and leg defects (Table 2, Fig. 7).

Discussion

Several important conclusions can be drawn from this study. First, it strengthens previous findings that cell culture results often vary from in vivo results at the organismal level. Two, regulation of mRNA degradation through the 3′UTR could involve sequences from the entire 3′UTR, not just the mRNA-degradation elements. Third, loss or gain of function mutant phenotypes could vary significantly depending upon parental genotype. While this study looked at specific parental genotypes carrying balancer chromosomes modifying *mid* mutant phenotypes in F1 progeny, this parental effect might likely extend to any genotype(s), with or without the balancers. This has implications for understanding any mutant phenotypes. Therefore, our results should help increase the rigor of studies and accuracy of results across the field and contribute to strategies that would mitigate differences in phenotypes in homozygous/F1 progeny because of parental chromosome effects.

Posttranscriptional regulation of *mid*

While a very tight regulation of *mid* at the posttranscriptional level by destroying the *mid*-mRNA occurs in S2 cells in culture (Fig. 1, b and c), where *mid* is not normally expressed, no such mRNA degradation was seen at the organismal level in cells where it is expressed (Fig. 3). Its regulation in cells and tissues where *mid* is not normally expressed at the organismal level was nuanced although the transgene lacking the entire 3′UTR showed a better stability than the one with it (Figs. 5 and 6 and Tables 1 and 2). A strong regulation may occur in vivo in some cells that we have not yet examined. For example, the endogenous *mid* gene appears to generate at

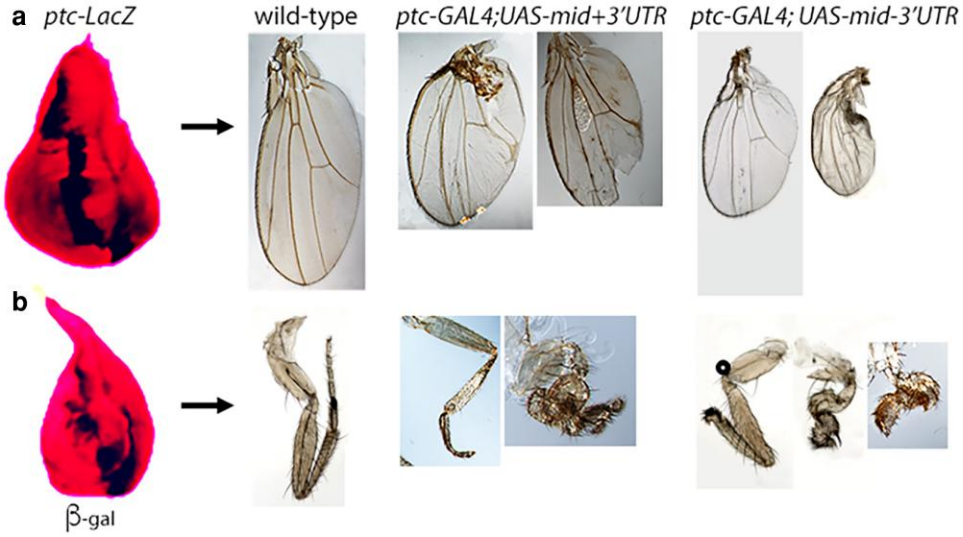

Fig. 7. Ectopic expression of *mid* with and without the 3′UTR causes wing and leg defects. The *ptc*-GAL4 driver-induced expression of *mid* with and without the 3′UTR caused wing (a) and leg (b) defects. Leg defects were more severe with the transgene that did not carry the 3′ UTR. The *ptc*-GAL4 expression domain in the wing and leg discs is also shown by inducing the UAS-lacZ transgene and monitoring the β-Gal expression. Differences in the penetrance or severity of the defects between the transgenes were not statistically significant.

Table 1. Viability of *ptc*-GAL4/UAS-*mid* with or without the 3′UTR progeny when cross is set with *ptc*-GAL4 over different balancers.

	Crossed with *ptc*-GAL4/CyoKrGAL4, UAS-GFP*		Crossed with *ptc*-GAL4/InGlaBc	
Genotype of the progeny	**% emergence at 18°C**	**% emergence at 20°C**	**% emergence at 18°C**	**% emergence at 20°C**
ptc-GAL4/UAS-*mid* +3′UTR	Lethal (0; N = 79)	Lethal (0; N = 52)	27.9 (N = 111)	Lethal (N = 145)
ptc-GAL4/UAS-*mid* -3′UTR	Lethal (0; N = 94)	Lethal (0; N = 100)	2.6 (N = 78)	Lethal (N = 110)

The total number of progeny flies (including those with balancer) examined is represented by N. Star indicates the genotype we had used in all the other experiments.

Table 2. Wing and leg defects in F1 flies from *mid*-transgenes with and without the 3′UTR at 2 different temperatures induced by the *ptc*-GAL4 driver in 2 different balancer backgrounds.

Wing defects			
	Crossed with *ptc*-GAL4/CyoKrGAL4, UAS-GFP		Crossed with *ptc*-GAL4/InGlaBc
Genotype of progeny	**% flies with wing defects at 18°C**	**% flies with wing defects at 20°C**	**% flies with wing defects at 18°C**
ptc-GAL4/UAS-*mid* +3′UTR	Lethal	Lethal	29.03 (N = 31)
ptc-GAL4/UAS-*mid* −3′UTR	Lethal	Lethal	50 (N = 78)
Leg defects			
	Crossed with ptc-GAL4/CyoKrGAL4, UAS-GFP		Crossed with ptc-GAL4/InGlaBc
Genotype of the progeny	**% flies with leg defects at 18°C**	**% flies with leg defects at 20°C**	**% flies with leg defects at 18°C**
ptc-GAL4/UAS-*mid* +3′UTR	Lethal	Lethal	22.6 (N = 31)
ptc-GAL4/UAS-*mid* −3′UTR	Lethal	Lethal	50 (N = 78)

The 2 different balancers are CyO and In(2LR) Gla, and Bc. N represents the *ptc*-GAL4/UAS-*mid*-progeny only.

least 2 different transcripts in vivo, one with a long 3′UTR, and the other with a short 3′UTR (see Supplementary Fig. 1, a and b, File 1). While the long 3′UTR has all the mRNA-degradation elements, the shorter one has only those that are part of the coding sequence and one element in the 3′UTR (our transgene without the 3′UTR carries only the one that is part of the coding sequence). Such a transcript might largely escape a 3′UTR-mediated degradation, as appears to be the case in cell culture and to a lesser extent in the imaginal discs. Perhaps this mRNA-degradation mechanism for *mid* (or other genes) evolved to destroy their inappropriate expression in certain cell types. This is evident in MP2 cells where an inappropriate expression of *mid* results in lineage defects (Fig. 4; see also Gaziova *et al.* 2020). At the same time, the presence of *mid*-transcripts with and without the 3′UTR suggests this differential mRNA processing perhaps arose for a reason: for mRNA degradation-mediated gene regulation to fine-tune its level, and to escape such a regulation. A cell-type and tissue-specific analysis of *mid*-transcripts for the long and short 3′UTR mRNA species is needed to determine if there is a tissue/cell-type-specific generation of one or the other or both of these transcripts.

Additionally, our results from the transgene that carried deletion of all the degradation elements from the 3′UTR indicate that while these elements contribute to the degradation of *mid*-mRNA (in S2 cells, with a *P* value 0.004), the remainder of the 3′UTR, which is highly AT-rich, likely participates in the degradation process (see Fig. 1d). Because the difference between the transgene with the 3′ UTR containing all the degradation elements (CHECK2-DE, Fig. 1d) and the one that carried the deletions for the degradation elements (CHECK2-NDE) was not highly significant (*P* value 0.12, Fig. 1d).

The differences in the effects between the 2 transgenes in transgenic experiments do not appear to be related to the site of their insertion. For example, the RNA in situ and protein-analysis results from the overexpression of the 2 transgenes in the MP2 lineage and the ectopic expression in the wing and leg discs indicate that the site of insertion of the transgenes does not necessarily influence negatively or positively between the 2 transgenes. In MP2, both the transgenes are expressed at similar levels. Besides, the 2 transgenes were induced by the same GAL4 driver. Caveats, however, exist; we cannot entirely rule out chromosomal influence. The temperature-dependent differences in transcription of the 2 transgenes or the phenotypic effects (see Fig. 6) are likely because the GAL4 protein is less active at lower temperatures (Brand *et al.* 1994) and the amount of transcription of the UAS-*mid* gene by the GAL4 is reduced at a lower temperature.

Regulation of Mid: translational repression vs protein degradation

The regulation of expression of Mid in MP2 appears to be posttranslational since both with and without the 3′UTR transgenes elicited the same level of *mid*-mRNA expression (Fig. 3a), protein expression as well as the penetrance of the phenotype (Figs. 3 and 4). Since MP2 is sensitive to Mid-levels and it is tightly regulated in that lineage (Gaziova *et al.* 2020), the posttranslational regulation prevents Mid overexpression in MP2. The regulation of *mid* at the translational level may occur in those cells where the endogenous *mid* is expressed and regulated. In those cells where the endogenous *mid* is not expressed, the regulation of ectopically expressed *mid* appears to be nuanced, parental genotype-dependent, and not translational. Thus, our results present a complex picture of the regulation of *mid* in vivo and how it might be regulated in the event of an inappropriate ectopic expression in conditions such as cancer.

A posttranscriptional process that mediates the downregulation of a protein could be from translational repression or protein degradation. Translational control could occur via a 5′UTR (Davuluri *et al.* 2000; Pickering and Willis 2005; Ringner and Krogh 2005; Araujo *et al.* 2012; Gu *et al.* 2014; Choi *et al.* 2017) with secondary structures of the 5′UTR, especially near the cap site, playing a role (Pickering and Willis 2005; Ringner and Krogh 2005; Gu *et al.* 2014). Analysis of the 5′UTR of *mid*, which is about 270 bases, using RNA-structure finder programs (http://rna.urmc.rochester.edu/RNAstructureWeb/Results.php?id=AllSub/20200819.210716-04f9e2c7) revealed that the 5′UTR of *mid*-transcripts has a prominent secondary structure (Supplementary Fig. 3, File 1). However, we do not know if this predicted structure exists in vivo and if it would interfere with the translation. A second possibility is that, as indicated by previous studies (Araujo *et al.* 2012; Choi *et al.* 2017), the binding of 5′UTR by RBPs could suppress translation. The presence of upstream open reading frames and upstream start codons could also suppress translation. The RBP-binding sequences appear to have the following composition: UGC(A/U)(A/U)NU. The *mid*-5′UTR has at least one RBP-binding site at position 164: TGCATCT (Supplementary Fig. 3, File 1). It also has an open reading frame with one AUG start codon at position 163. A 5′UTR deletion and analysis of transgenic lines carrying such deletion is essential to determine if 5′UTR-mediated translational repression occurs with the *mid*-transcript.

Cell culture vs organismal analysis

Tissue culture cells have been extensively used for the expression of reporter fusions and transgenes in gene expression studies. However, often posttranscriptional and translational regulation of gene expression is found to differ between tissue culture cells and in an organism. For example, differences in gene expression were observed between in vivo and in vitro conditions for mammalian neuronal cell types, which is thought to be due to perturbations in signaling pathways in cultured cells (LoVerso *et al.* 2015). A comparison of gene expression profiles between retina in vivo and cultured retinal explants showed similarity in expression of the majority of genes, although the retinal explants showed a decrease in the expression of genes such as cyclin D1 (Liu *et al.* 2008). This might be because of a lack of external factors that maintain *cyclin D1* expression in retinal explants.

Another example is the full-length Dorsal protein, which when expressed in S2 cells accumulates mostly in the cytoplasm as seen in early embryos of Drosophila (Rushlow *et al.* 1989). However, the truncated Dorsal protein that lacks the 6 amino acids in the C-terminal localizes to the nucleus in S2 cells. Another study on nuclear localization of the Dorsal protein showed that in S2 cells, the serine residue at Position 312 of the Dorsal protein controlled its nuclear localization and transcriptional activity (Drier *et al.* 1999). The same mutant Dorsal protein, however, showed a normal nuclear localization, formed a gradient, and mediated the dorsal–ventral patterning of the embryo (Briggs *et al.* 1998; Drier *et al.* 1999). The significant difference in the posttranscriptional mRNA regulation of *mid* between cells in culture and in the organism is yet another example of the artificial nature of the cell culture system. Cells in culture have aneuploidy, as well as lack context, affecting protein degradation, autophagy, and signaling events, all of which could mediate the difference (Oromendia and Amon 2014).

There are many examples of a 3′UTR-mediated regulation via degradation of mRNA. The low-density lipoprotein receptor LDLR mRNA stability with cell-type/tissue specificity and its activity is positively correlated with cellular levels of hnRNP D p37 isoform (Singh *et al.* 2014). It has been proposed that the varying levels of ARE BP (AU-rich element binding proteins) between cell types/tissues may determine the turnover rate of the mRNA containing AU-rich elements in its 3′UTR. For example, the LDLR mRNA contains 3 AU-rich elements in its 2.5 kb long 3′UTR, which mediates rapid turnover rate in liver cells. However, the cardiac cells have a longer half-life of LDLR mRNA than liver cells. The stability of the LDLR mRNA in these cell/tissue types was inversely related to the abundance of hnRNP D (Singh *et al.* 2014). The UC-rich DICE or Differentiation control elements present in the 3′UTR can also control mRNA stability. For example, the 15-lipoxygenase mRNA is abundant in bone marrow erythroid precursor cells but is transcriptionally repressed until they become mature erythrocytes. DICE-binding proteins such as hnRNP E1 and hnRNP K bind to UC-rich sequences and mediate translational repression of the mRNA (Ostareck-Lederer *et al.* 1994; Ostareck *et al.* 1997). Our results indicate that *mid* is another example where its 3′UTR mediates destruction of its mRNA, but only in cell culture.

It is intriguing that although the 3′UTR of *mid* has strong mRNA degradation elements, a 3′UTR that is highly enriched with

AT-sequence even when lacking the "degradation" elements also could mediate mRNA degradation (Fig. 1d). It is also intriguing that despite the 3′UTR having strong mRNA-degradation elements, it is not degraded in the organism itself where *mid* is expressed, at least in certain cells we have examined (Fig. 3). Thus, having degradation sequences does not guarantee that degradation will occur, especially at the organismal level. However, in cells or tissues where *mid* is not normally expressed such as wing or the *ptc*-domain of leg discs (Fig. 5a, Supplementary Figs. 4 and 5, File 1), ectopic expression of the *mid*-transgene without the 3′UTR had better stability than the one with the 3′UTR (Figs. 5 and 6; Tables 1 and 2; see also Fig. 1d). But this regulation was not as strong as in cell culture. We certainly are not arguing that cell culture systems or bioinformatics have limited use, they certainly help streamline investigative approaches, but they do not substitute for biological explorations using organisms and understand what occurs at the organismal level.

The 3′UTR-dependent transgenerational effects of balancers

One of the interesting findings from this study is that there was a transgenerational parental balancer-induced modifier effect on mRNA regulation (Tables 1 and 2). With one balancer in one of the parents, there was lethality at the F1 progeny level, and no adults emerged in either of the transgenic lines (with or without the 3′UTR) when induced in discs, whereas with another balancer, viable F1 adults were observed with both the transgenes. However, the transgene without the 3′UTR had a stronger effect with only a few adults emerging, indicating that it was not subjected to mRNA-degradation regulation (Tables 1 and 2).

This effect is not likely from second-site mutations on chromosomes that carry the transgenes but is an example of how balancers influence phenotypes in progeny flies, a transgenerational effect. This is important, physiological or not, for all fly researchers since it has the potential to skew results depending on the balancers they use. It can contribute to reproducibility problems. Indeed, we had shown a similar example in one of our previous studies (Gaziova and Bhat 2009). This is also an opportunity for reminding the community to be aware of the potential caveats of balancer chromosome effects (see also Miller *et al.* 2019). We generally ascertain a phenotype with and without a balancer and rely more on the penetrance of the phenotype on a genotype that did not carry a balancer in parents. In summary, our results provide intriguing insights into the complex regulation of the expression of this important gene during development. Our results show that tissue culture system often does not apply to organisms and the entire parental genotype matters in modifying/skewing/altering phenotype(s) of a mutation in homozygous mutant progeny.

Data availability

Strains and plasmids are available upon request. The authors affirm that all data necessary for confirming the conclusions of the article are present within the paper, figures, tables, and Supplementary data. The Supplementary datasets contain *mid* sequence, supplementary figures, methodology, and raw data relevant to tables, qPCR, and figures presented in the paper.

Supplemental material available at GENETICS online.

Acknowledgments

We would like to thank Drs John Reinitz for the anti-Odd antibody, the Bloomington Stock center for various fly lines, and Jim Skeath for the AJ96 enhancer-trap line. KMB appreciates the support from Dr. Jin Mo Chung, and the Department of Neuroscience and Cell Biology, University of Texas Medical Branch, Galveston, Texas, where a significant part of this project was initiated.

Funding

This work is supported by a grant from the National Institutes of Health grants GM127478 and NS131315 to KMB.

Conflicts of interest

The author(s) declare no conflicts of interest.

Literature cited

Amor-Salamanca A, Santana Rodriguez A, Rasoul H, Rodriguez-Palomares JF, Moldovan O, Hey TM, Delgado MG, Cuenca DL, de Castro Campos D, Basurte-Elorz MT *et al.* 2024. Role of TBX20 truncating variants in dilated cardiomyopathy and left ventricular noncompaction. Circ Genom Precis Med. 17(2):e004404. doi:10.1161/CIRCGEN.123.004404.

Araujo PR, Yoon K, Ko D, Smith AD, Qiao M, Suresh U, Burns SC, Penalva LO. 2012. Before it gets started: regulating translation at the 5′ UTR. Comp Funct Genomics. 2012:475731. doi:10.1155/2012/475731.

Bamshad M, Lin RC, Law DJ, Watkins WC, Krakowiak PA, Moore ME, Franceschini P, Lala R, Holmes LB, Gebuhr TC *et al.* 1997. Mutations in human TBX3 alter limb, apocrine and genital development in ulnar-mammary syndrome. Nat Genet. 16(3):311–315. doi:10.1038/ng0797-311.

Basson CT, Huang T, Lin RC, Bachinsky DR, Weremowicz S, Vaglio A, Bruzzone R, Quadrelli R, Lerone M, Romeo G *et al.* 1999. Different TBX5 interactions in heart and limb defined by Holt-Oram syndrome mutations. Proc Natl Acad Sci U S A. 96(6):2919–2924. doi:10.1073/pnas.96.6.2919.

Bhat KM. 1996. The patched signaling pathway mediates repression of gooseberry allowing neuroblast specification by wingless during Drosophila neurogenesis. Development. 122(9):2921–2932. doi:10.1242/dev.122.9.2921.

Bhat KM. 1999. Segment polarity genes in neuroblast formation and identity specification during Drosophila neurogenesis. Bioessays. 21(6):472–485. doi:10.1002/(SICI)1521-1878(199906)21:6<472::AID-BIES4>3.0.CO; 2-W.

Brand AH, Manoukian AS, Perrimon N. 1994. Ectopic expression in Drosophila. Methods Cell Biol. 44:635–654. doi:10.1016/s0091-679x(08)60936-x.

Brand AH, Perrimon N. 1993. Targeted gene expression as a means of altering cell fates and generating dominant phenotypes. Development. 118(2):401–415. doi:10.1242/dev.118.2.401.

Briggs LJ, Stein D, Goltz J, Corrigan VC, Efthymiadis A, Hubner S, Jans DA. 1998. The cAMP-dependent protein kinase site (Ser312) enhances dorsal nuclear import through facilitating nuclear localization sequence/importin interaction. J Biol Chem. 273(35):22745–22752. doi:10.1074/jbc.273.35.22745.

Carlson H, Ota S, Song Y, Chen Y, Hurlin PJ. 2002. Tbx3 impinges on the p53 pathway to suppress apoptosis, facilitate cell transformation and block myogenic differentiation. Oncogene. 21(24):3827–3835. doi:10.1038/sj.onc.1205476.

Chang F, Xing P, Song F, Du X, Wang G, Chen K, Yang J. 2016. The role of T-box genes in the tumorigenesis and progression of cancer. Oncol Lett. 12(6):4305–4311. doi:10.3892/ol.2016.5296.

Choi S, Park C, Kim KE, Kim KK. 2017. An in vitro technique to identify the RNA binding-site sequences for RNA-binding proteins. Biotechniques. 63(1):28–33. doi:10.2144/000114567.

Davuluri RV, Suzuki Y, Sugano S, Zhang MQ. 2000. CART classification of human 5′ UTR sequences. Genome Res. 10(11): 1807–1816. doi:10.1101/gr.gr-1460r.

Doe CQ. 1992. Molecular markers for identified neuroblasts and ganglion mother cells in the Drosophila central nervous system. Development. 116(4):855–863. doi:10.1242/dev.116.4.855.

Drier EA, Huang LH, Steward R. 1999. Nuclear import of the Drosophila Rel protein Dorsal is regulated by phosphorylation. Genes Dev. 13(5):556–568. doi:10.1101/gad.13.5.556.

Fu CL, Wang XF, Cheng Q, Wang D, Hirose S, Liu QX. 2016. The T-box transcription factor midline regulates wing development by repressing wingless and hedgehog in Drosophila. Sci Rep. 6(1): 27981. doi:10.1038/srep27981.

Gaziova I, Bhat KM. 2009. Ancestry-independent fate specification and plasticity in the developmental timing of a typical Drosophila neuronal lineage. Development. 136(2):263–274. doi: 10.1242/dev.027854.

Gaziova I, Gazi M, Mar J, Bhat KM. 2020. Restriction on self-renewing asymmetric division is coupled to terminal asymmetric division in the Drosophila CNS. PLoS Genet. 16(9):e1009011. doi:10.1371/journal.pgen.1009011.

Gu W, Xu Y, Xie X, Wang T, Ko JH, Zhou T. 2014. The role of RNA structure at 5′ untranslated region in microRNA-mediated gene regulation. RNA. 20(9):1369–1375. doi:10.1261/rna.044792.114.

Kolodziej PA, Jan LY, Jan YN. 1995. Mutations that affect the length, fasciculation, or ventral orientation of specific sensory axons in the Drosophila embryo. Neuron. 15(2):273–286. doi:10.1016/0896-6273(95)90033-0.

Lai EC, Posakony JW. 1997. The Bearded box, a novel 3′ UTR sequence motif, mediates negative post-transcriptional regulation of Bearded and Enhancer of split Complex gene expression. Development. 124(23):4847–4856. doi:10.1242/dev.124.23.4847.

Li QY, Newbury-Ecob RA, Terrett JA, Wilson DI, Curtis AR, Yi CH, Gebuhr T, Bullen PJ, Robson SC, Strachan T *et al.* 1997. Holt-Oram syndrome is caused by mutations in TBX5, a member of the Brachyury (T) gene family. Nat Genet. 15(1):21–29. doi:10.1038/ng0197-21.

Liu MG, Li H, Xu X, Barnstable CJ, Zhang SS. 2008. Comparison of gene expression during in vivo and in vitro postnatal retina development. J Ocul Biol Dis Infor. 1(2–4):59–72. doi:10.1007/s12177-008-9009-z.

Livak KJ, Schmittgen TD. 2001. Analysis of relative gene expression data using real-time quantitative PCR and the 2(−Delta Delta C(T)) Method. Methods. 25(4):402–408. doi:10.1006/meth.2001.1262.

LoVerso PR, Wachter CM, Cui F. 2015. Cross-species transcriptomic comparison of in vitro and in vivo mammalian neural cells. Bioinform Biol Insights. 9:153–164. doi:10.4137/BBI.S33124.

Manavalan MA, Gaziova I, Bhat KM. 2013. The midline protein regulates axon guidance by blocking the reiteration of neuroblast rows within the Drosophila ventral nerve cord. PLoS Genet. 9(12):e1004050. doi:10.1371/journal.pgen.1004050.

Merscher S, Funke B, Epstein JA, Heyer J, Puech A, Lu MM, Xavier RJ, Demay MB, Russell RG, Factor S *et al.* 2001. TBX1 is responsible for cardiovascular defects in velo-cardio-facial/DiGeorge syndrome. Cell. 104(4):619–629. doi:10.1016/s0092-8674(01)00247-1.

Miller DE, Cook KR, Hawley RS. 2019. The joy of balancers. PLoS Genet. 15(11):e1008421. doi:10.1371/journal.pgen.1008421.

Nusslein-Volhard C, Wieschaus E, Kluding H. 1984. Mutations affecting the pattern of the larval cuticle in Drosophila melanogaster: I. Zygotic loci on the second chromosome. Wilehm Roux Arch Dev Biol. 193(5):267–282. doi:10.1007/BF00848156.

Oromendia AB, Amon A. 2014. Aneuploidy: implications for protein homeostasis and disease. Dis Model Mech. 7(1):15–20. doi:10.1242/dmm.013391.

Ostareck DH, Ostareck-Lederer A, Wilm M, Thiele BJ, Mann M, Hentze MW. 1997. mRNA silencing in erythroid differentiation: hnRNP K and hnRNP E1 regulate 15-lipoxygenase translation from the 3′ end. Cell. 89(4):597–606. doi:10.1016/s0092-8674(00)80241-x.

Ostareck-Lederer A, Ostareck DH, Standart N, Thiele BJ. 1994. Translation of 15-lipoxygenase mRNA is inhibited by a protein that binds to a repeated sequence in the 3′ untranslated region. EMBO J. 13(6):1476–1481. doi:10.1002/j.1460-2075.1994.tb06402.x.

Pickering BM, Willis AE. 2005. The implications of structured 5′ untranslated regions on translation and disease. Semin Cell Dev Biol. 16(1):39–47. doi:10.1016/j.semcdb.2004.11.006.

Prince S, Carreira S, Vance KW, Abrahams A, Goding CR. 2004. Tbx2 directly represses the expression of the p21(WAF1) cyclin-dependent kinase inhibitor. Cancer Res. 64(5):1669–1674. doi:10.1158/0008-5472.can-03-3286.

Qian L, Liu J, Bodmer R. 2005. Neuromancer Tbx20-related genes (H15/midline) promote cell fate specification and morphogenesis of the Drosophila heart. Dev Biol. 279(2):509–524. doi:10.1016/j.ydbio.2005.01.013.

Ringner M, Krogh M. 2005. Folding free energies of 5′-UTRs impact post-transcriptional regulation on a genomic scale in yeast. PLoS Comput Biol. 1(7):e72. doi:10.1371/journal.pcbi.0010072.

Rushlow CA, Han K, Manley JL, Levine M. 1989. The graded distribution of the dorsal morphogen is initiated by selective nuclear transport in drosophila. Cell. 59(6):1165–1177. doi:10.1016/0092-8674(89)90772-1.

Savant-Bhonsale S, Cleveland DW. 1992. Evidence for instability of mRNAs containing AUUUA motifs mediated through translation-dependent assembly of a > 20S degradation complex. Genes Dev. 6(10):1927–1939. doi:10.1101/gad.6.10.1927.

Singh AB, Li H, Kan CF, Dong B, Nicolls MR, Liu J. 2014. The critical role of mRNA destabilizing protein heterogeneous nuclear ribonucleoprotein d in 3′ untranslated region-mediated decay of low-density lipoprotein receptor mRNA in liver tissue. Arterioscler Thromb Vasc Biol. 34(1):8–16. doi:10.1161/ATVBAHA.112.301131.

Svendsen PC, Ryu JR, Brook WJ. 2015. The expression of the T-box selector gene midline in the leg imaginal disc is controlled by both transcriptional regulation and cell lineage. Biol Open. 4(12): 1707–1714. doi:10.1242/bio.013565.

Tautz D, Pfeifle C. 1989. A non-radioactive in situ hybridization method for the localization of specific RNAs in Drosophila embryos reveals translational control of the segmentation gene hunchback. Chromosoma. 98(2):81–85. doi:10.1007/BF00291041.

Wilk R, Hu J, Krause HM. 2017. In situ hybridization: fruit fly embryos and tissues. Curr Protoc Essent. Lab Tech. 15:9.3.1–9.3.26. doi:10.1002/cpet.14.

Editor: N. Perrimon